



PERGAMON

Journal of Quantitative Spectroscopy &  
Radiative Transfer 82 (2003) 401–412

Journal of  
Quantitative  
Spectroscopy &  
Radiative  
Transfer

[www.elsevier.com/locate/jqsrt](http://www.elsevier.com/locate/jqsrt)

## Total internal partition sums for molecular species in the 2000 edition of the HITRAN database

J. Fischer<sup>a</sup>, R.R. Gamache<sup>a,\*</sup>, A. Goldman<sup>b</sup>, L.S. Rothman<sup>c</sup>, A. Perrin<sup>d</sup>

<sup>a</sup>*Department of Environmental, Earth, and Atmospheric Sciences, University of Massachusetts Lowell,  
Lowell, MA 01854, USA*

<sup>b</sup>*Department of Physics, University of Denver, Denver, CO 80208, USA*

<sup>c</sup>*Atomic and Molecular Physics Division, Harvard-Smithsonian Center for Astrophysics, Cambridge,  
MA 02138, USA*

<sup>d</sup>*Laboratoire de Photophysique Moléculaire, Université Paris Sud, 91405 Orsay, France*

Received 28 January 2003; received in revised form 26 March 2003; accepted 27 March 2003

### Abstract

Total internal partition sums (TIPS) are calculated for all molecular species in the 2000 HITRAN database. In addition, the TIPS for 13 other isotopomers/isotopologues of ozone and carbon dioxide are presented. The calculations address the corrections suggested by Goldman et al. (JQSRT 66 (2000) 455). The calculations consider the temperature range 70–3000 K to be applicable to a variety of remote sensing needs. The method of calculation for each molecular species is stated and comparisons with data from the literature are discussed. A new method of recall for the partition sums, Lagrange 4-point interpolation, is developed. This method, unlike previous versions of the TIPS code, allows all molecular species to be considered.

© 2003 Elsevier Ltd. All rights reserved.

**Keywords:** Total internal partition sums; Partition functions; Atmospheric molecular species; HITRAN; Temperature dependence of partition functions

### 1. Overview

The aim of this work has been to provide a comprehensive set of total internal partition sums (TIPS) for species of atmospheric interest, calculated to the greatest possible degree of accuracy and packaged in a form which allows for easy and rapid recall of the data. This work is therefore a modern revision of previous calculations which supplants previously released partition function data. As such, the work is based upon prior work by Gamache et al. [1,2] and incorporates all of

\* Corresponding author. Tel.: +1-978-934-3904; fax: +1-978-934-3069.

E-mail address: [robert.gamache@uml.edu](mailto:robert.gamache@uml.edu) (R.R. Gamache).

the corrections discussed in Goldman et al. [3], as well as newer physical constants and molecular parameters.

Given that partition functions are most commonly used by those interested in remote sensing, these partition functions are provided to augment the HITRAN 2000 spectroscopic database [4]. Therefore, the scope of the calculations matches these interests. Partition functions are provided for all molecular species and isotopologues present on the 2000 edition of the HITRAN database, except for the O atom, for which rotational and vibrational partition functions are undefined. Additionally, partition functions are provided for a number of ozone isotopologues/isotopomers which are not currently on the HITRAN database and one isotopologue of carbon dioxide. The temperature range of the calculations (70–3000 K) was selected to match a variety of remote sensing needs (planetary atmospheres, combustion gases, plume detection, etc.). Although there are a number of molecular species for which the partition sum at high temperatures is of no practical importance, e.g. ozone, hydrogen peroxide, the aim was to have a consistent set of partition sums for all molecular species.

## 2. Methodology

The general methodology used in this study was selected to minimize the possibility of human error or faulty constants producing error in the final partition sums. Molecular constants used were taken from scientific literature. The total internal partition sum is given by a sum over all states,  $s$ , labeled by the electronic, vibrational, rotational, torsional, ... structure of the molecule,

$$Q(\text{elec}, \text{vib}, \text{rot}, \text{tors}, \dots) = d_i \sum_{\text{all states } s} d_s e^{-E_s/kT}, \quad (1)$$

where  $d_i$  is the state-independent degeneracy factor and  $d_s$  is the state-dependent degeneracy factor (see below and [2]) and  $E_s$  is the energy of the electronic, vibrational, rotational, torsional, ... state. In practice, the energy states are usually not known for all rotational levels of all vibrational states of all electronic states. When there are other complications, such as lambda doubling, torsional motion, etc. the situation for the energy states is worse. In such cases it is assumed that

$$E(\text{elec}, \text{vib}, \text{rot}, \text{tors}, \dots) = E_{\text{elec}} + E_{\text{vib}} + E_{\text{rot}} + E_{\text{tors}} + \dots \quad (2)$$

from which the product approximation can be made

$$Q(\text{elec}, \text{vib}, \text{rot}, \text{tors}, \dots) = Q_{\text{elec}} \times Q_{\text{vib}} \times Q_{\text{rot}} \times Q_{\text{tors}} \times \dots \quad (3)$$

The problem is now reduced to calculating the electronic, vibrational, rotational, ... partition sums. Which approach is used is determined by the availability of energy states for the molecule in question.

For the rotational partition sums, when possible, rotational energy levels were calculated from molecular constants using appropriate expressions and compared to measured energy levels. For certain species, energy levels were provided by other researchers. These energy levels were then used to evaluate the rotational partition sum at a variety of temperatures by direct summation of

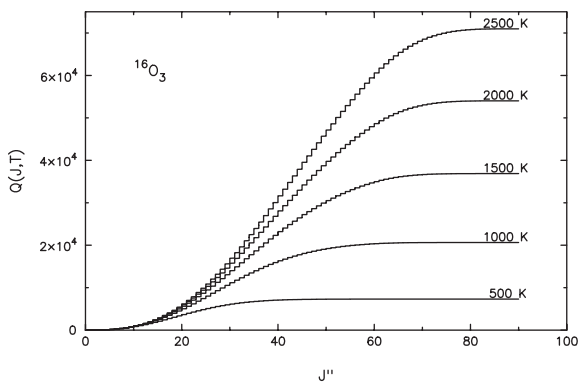


Fig. 1. Convergence of the partition sum as a function of temperature for  $^{16}\text{O}_3$ .

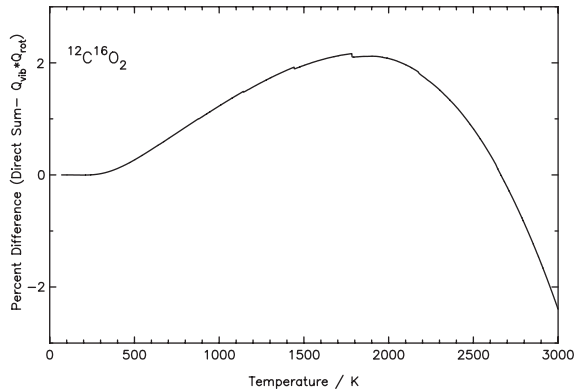


Fig. 2. Comparison of the product approximation,  $Q_{\text{vib}} * Q_{\text{rot}}$ , with  $Q_{\text{Direct Sum}}$  for  $^{12}\text{C}^{16}\text{O}_2$ .

the expression

$$Q_{\text{rot}} = d_i \sum_{\text{all rotational states}} d_r e^{-E_r/kT}, \quad (4)$$

where  $d_r$  is the degeneracy of the rotational state with energy  $E_r$ . This sum clearly becomes incomplete at high enough temperatures for a given set of energies. Therefore, the convergence of these partition sums was tested by plotting  $Q_{\text{rot}}(T,J)$  versus the rotational quantum number  $J$  at various temperatures of interest. Converged partition sums exhibit a horizontal asymptote at energy levels where  $E_r$  is significantly larger than  $kT$  cease to contribute significantly to the sum. Incomplete partition sums do not exhibit this asymptote. By finding the greatest temperature at which these plots still exhibited an asymptote, it was possible to determine the highest temperature to which a direct sum could be used for a given set of energies. Fig. 1 is a convergence plot for the  $^{16}\text{O}_3$  species. The general trend of all convergence plots is similar to this graph. For a given temperature, lower rotational energy levels contribute significantly more to the partition sum, due to the  $e^{-E_r/kT}$  term. At a constant temperature, as higher rotational levels are summed, they contribute less and less to the total internal partition function and a horizontal asymptote is seen in the graph. However, at higher temperatures, it is impossible to reach this point with a finite set of rotational energy levels. The highest temperature at which the graph still exhibits a horizontal asymptote (i.e. the point where summation of all higher energy levels leads to a negligible change in the total value of the partition sum) is the highest temperature at which the partition sum remains converged.

Next, when necessary, an appropriate analytical expression was used to evaluate  $Q_{\text{rot}}(T)$ . The expression used was selected based on molecular symmetry. For linear molecules, McDowell's expression was used [5]; for asymmetric rotors, Watson's expression was used [6], for spherical [7] and symmetric top molecules [8], McDowell's expressions were used.

A comparison was then performed between the direct sum and the analytical expression for each species. Bearing in mind that the direct sum is only accurate at temperatures low enough for it to remain converged and that all of the analytical expressions used are approximations which become

better in the limit of high temperatures, the assumption was made that if a good agreement can be demonstrated between a converged direct sum and an analytical expression for a fair temperature range, that the analytical expression probably exhibits similar or smaller errors at higher temperatures. In all cases, a good agreement could be demonstrated between the two methods and, in most cases, the analytical expression was used for the entire temperature range. For certain species where the analytical expression did not work as well for lower temperatures, the direct sum was used for low temperatures and an analytical expression was used for higher temperatures.

For all species, unless otherwise noted, the vibrational partition function was calculated using the harmonic oscillator approximation (HOA) of Herzberg [9]. Vibrational fundamentals were taken from the literature and used in the following expression:

$$Q_{\text{vib}}(T) = \prod_{\text{vibrational fundamentals}} \frac{1}{1 - e^{hcE_v/kT}}. \quad (5)$$

Once the vibrational and rotational partition functions were calculated for species in the electronic ground state and with no other structure (hyperfine, torsion, ...), the product approximation,  $Q_{\text{vib}} \times Q_{\text{rot}}$ , was used to evaluate the total internal partition functions. The product approximation assumes that the vibrational and rotational energy levels are totally independent of each other and therefore, that the rotational and vibrational partition functions are also totally independent. With this approximation, the total internal partition function, for most molecules, is merely the product of the rotational and vibrational partition functions. The validity of the product approximation was tested in a rough manner by comparing the total internal partition function for CO<sub>2</sub> calculated by using the product approximation with an analytical expression with a partition function calculated by a direct sum of ro-vibrational energy levels. The results of this test are summarized in Fig. 2.

One often neglected aspect of calculating partition sums is the inclusion of state independent degeneracy factors. Degeneracy factors can be divided into state dependent and state independent components. Note, below when the state dependent degeneracy factors are discussed here it is the factor in addition to the normal  $(2J + 1)$  or the  $(2F + 1)$  factor. These additional state dependent degeneracy factors occur in systems in which the rotational wavefunction of the species couple with the nuclear wavefunctions of some of the atoms in the molecule. Typically, this happens in species with some degree of symmetry where only certain products of rotational and nuclear wavefunctions yield the proper symmetry for the complete wavefunctions. The net result of this is that for some molecules, even and odd symmetry states have different weights and these values must be factored in accordingly when calculating partition sums.

For molecules where two identical nuclei are exchanged upon rotation, it is easy to determine the nuclear statistical weights which are part of the state dependent degeneracy factors. For Fermi systems (i.e. molecules where the exchanged nuclei have half-integer spins) and Bose systems (i.e. molecules where the exchanged nuclei have integer spins) the following equations give the state dependent degeneracy factors:

$$\begin{aligned} \text{Fermi system--even state: } & \frac{1}{2}[(2I_x + 1)^2 - (2I_x + 1)], \\ \text{Bose system--odd state: } & \frac{1}{2}[(2I_x + 1)^2 - (2I_x + 1)], \\ \text{Fermi system--odd state: } & \frac{1}{2}[(2I_x + 1)^2 - (2I_x + 1)], \\ \text{Bose system--even state: } & \frac{1}{2}[(2I_x + 1)^2 - (2I_x + 1)], \end{aligned} \quad (6)$$

where  $I_x$  is the nuclear spin of the atoms which are interchanged. For example, for  $\text{H}_2\text{O}$ , the two interchanged nuclei are the hydrogen atoms, which are spin 1/2. Inserting this value into the above equations gives a three-fold degeneracy for the odd states and a one-fold degeneracy for the even states. For  $^{16}\text{O}_3$ , the two interchanged nuclei are oxygen atoms with spin zero. Substituting this value into the above equations yields a one-fold degeneracy for the even levels and a zero-fold degeneracy for the odd levels (i.e., such levels do not exist). For molecules which have more than one pair of atoms exchanged upon rotation, expressions for the number of spin functions for each state are given in Ref. [9, p. 17, Eqs. (I.8) and (I.9)].

When direct sums were calculated in this work, state dependent factors were handled explicitly by calculating the parity of each state using an expression appropriate for the molecular symmetry of the species involved and the correct degeneracy factors were incorporated into the direct sum. When analytical expressions were used, an average state dependent factor was used by taking the arithmetic mean of the state dependent factors involved. For example, for  $^{16}\text{O}_3$ , a factor of 0.5 was used to account for the average of the state dependent factors.

State independent factors are often omitted from partition sum calculations. They are, however, necessary for the partition functions to relate to thermodynamic quantities. State independent factors occur in molecules where there are atoms with non-zero nuclear spins that are not interchanged upon rotation. This degeneracy factor is expressed as  $\prod(2I+1)$ , where  $I$  is the nuclear spin and the product is taken over all nuclei not interchanged by rotation [9]. Note, there are other factors that can sometimes mimic state independent factors, for example a doubling for all levels when there is lambda doubling, torsion or inversion. These factors are discussed specifically in the appropriate sections of the text.

Although the state independent factors are often omitted in studies which report partition sums, it is usually not a problem, since the actual values of the partition sum are infrequently used. More commonly, a ratio of partition sums is employed and the state independent factors cancel out. However, in this study, every attempt has been made to include the complete state independent factor for all species and hence determine the true total internal partition function. In comparing the partition sums from this study to others from the literature, it is sometimes necessary to multiply by an integer value to obtain agreement due to the omission of the state-independent factors in other studies. Such comparisons are discussed specifically in the text.

### 3. Calculations

The calculations of the total internal partition sums were made employing a number of methodologies depending on the molecular species in question. Here, the calculations are summarized. Ref. [10] gives complete details of the calculations including the rotational and vibrational constants used, the state-independent and state-dependent statistical factors, complications that arise due to hyperfine structure, lambda doubling, spin coupling, etc., comparisons of the direct sum and analytical calculations, and the accuracy of the recall of the calculated values. In addition, the analytical models for  $Q_{\text{rot}}$  that were developed are presented in Ref. [10].

Because of the temperature range of the study, 70–3000 K, it was necessary to make most of the calculations via the product approximation and determine  $Q_{\text{rot}}$  via analytical models and  $Q_{\text{vib}}$  via the harmonic oscillator approximation of Herzberg. There were a small number of species where

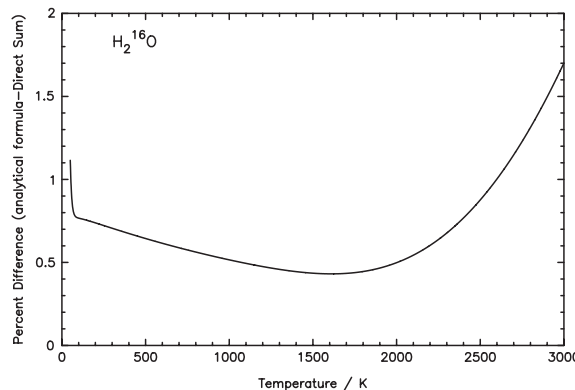


Fig. 3. Percent difference between  $Q_{\text{Direct Sum}}$  and  $Q_{\text{analytical formula}}$  for  $\text{H}_2^{16}\text{O}$ .

the direct sum over energy states yields the TIPS. These include the isotopologues of oxygen molecule and the isotopologues of the hydrogen halides. For the isotopologues of OH and  $\text{PH}_3$  the product approximation,  $Q_{\text{vib}} \times Q_{\text{rot}}$ , was used where  $Q_{\text{rot}}$  was determined by direct summation. For OH the rotational energy levels were produced using the method of Beaudet and Poynter [11], which includes fine structure interaction and lambda doubling.

The TIPS for all isotopologues/isotopomers of the following asymmetric rotors on the HITRAN database:  $\text{O}_3$ ,  $\text{SO}_2$ ,  $\text{NO}_2$ ,  $\text{HNO}_3$ ,  $\text{H}_2\text{CO}$ ,  $\text{HOCl}$ ,  $\text{COF}_2$ ,  $\text{H}_2\text{S}$ ,  $\text{HCOOH}$ ,  $\text{HO}_2$ ,  $\text{ClONO}_2$ ,  $\text{HOBr}$ , and  $\text{C}_2\text{H}_4$ , were determined by the product approximation,  $Q_{\text{vib}} \times Q_{\text{rot}}$ , where  $Q_{\text{rot}}$  was determined by the analytical formula of Watson [6]. For  $\text{NO}_2$  there were corrections for electron spin and hyperfine Fermi resonance (see [12]) and the analytical model for  $\text{HO}_2$  included an additional statistical factor of 2 in order to account for the  $F$ -splittings due to ESR present in this open shell molecule.

For water vapor, a light asymmetric rotor, comparisons were made between the  $Q_{\text{rot}}$  determined by direct sum and by using Watson's analytical model. Fig. 3 shows the difference between the direct sum and the analytical expression for the  $\text{H}_2^{16}\text{O}$  species for the temperature range 50–3000 K. The figure shows that the difference between the two methods is large at low temperature, where the analytical expression is unable to properly model the quantum structure of the system. The difference is also quite large at high temperatures, where the direct sum is incomplete. However, at intermediate temperatures, there is a region where the agreement between the two methods is quite good. In order to provide the most accurate representation of the partition sum, a combination of the direct sum and the analytical expression was used for  $Q_{\text{rot}}$  in the final product approximation partition sums for the four most abundant species. In part, this method was selected because the greatest errors for all of these species occurred at low temperatures. The lowest temperatures at which the analytical expression was used were 1401 K, 451 K, 349 K and 675 K for  $\text{H}_2^{16}\text{O}$ ,  $\text{H}_2^{18}\text{O}$ ,  $\text{H}_2^{17}\text{O}$ ,  $\text{HD}^{16}\text{O}$ , respectively. At these temperatures, the differences between the direct sum and the analytical expression were 0.62%, 0.52%, −0.46% and 0.66% for  $\text{H}_2^{16}\text{O}$ ,  $\text{H}_2^{18}\text{O}$ ,  $\text{H}_2^{17}\text{O}$ ,  $\text{HD}^{16}\text{O}$ , respectively. For  $\text{HD}^{18}\text{O}$  and  $\text{HD}^{17}\text{O}$  the product approximation with Watson's analytical model for  $Q_{\text{rot}}$  was used throughout the entire temperature range.

The product approximation,  $Q_{\text{vib}} \times Q_{\text{rot}}$ , with McDowell's model [5] was used for all isotopologues of the following linear molecules on the database:  $\text{CO}_2$ ,  $\text{N}_2\text{O}$ ,  $\text{CO}$ ,  $\text{OCS}$ ,  $\text{N}_2$ ,  $\text{HCN}$ ,  $\text{C}_2\text{H}_2$ , and  $\text{NO}^+$ .

The TIPS for isotopologues of the symmetric top molecules on the database; CH<sub>3</sub>D, NH<sub>3</sub>, CH<sub>3</sub>Cl, and C<sub>2</sub>H<sub>6</sub>, were calculated using the product approximation,  $Q_{\text{vib}} \times Q_{\text{rot}}$ , with  $Q_{\text{rot}}$  determined via the analytical formula of McDowell [8]. For <sup>12</sup>CH<sub>4</sub>, <sup>13</sup>CH<sub>4</sub>, and SF<sub>6</sub> the product approximation was used with  $Q_{\text{rot}}$  determined by McDowell's spherical top formula [7].

For the doublet-pi molecular species of NO and ClO, which have spin-orbit, lambda doubling and hyperfine interactions (see Ref. [3] for details) the product approximation,  $Q_{\text{vib}} \times Q_{\text{rot}}$ , was used. An analytical formula, based on the linear molecule formula of McDowell [5], was developed. Factors of 3, 3, and 2 for the hyperfine structure and 2, 2, and 2, for the lambda doubling structure were incorporated into the analytical partition sums for <sup>14</sup>N<sup>16</sup>O, <sup>14</sup>N<sup>18</sup>O, and <sup>15</sup>N<sup>16</sup>O, respectively. For both isotopologues of ClO, the analytical partition sums were multiplied by 4 to account for the hyperfine structure and 2 to account for the lambda doubling.

An analytical model for the rotational partition sum, which accounts for torsion in hydrogen peroxide, was developed using a number of approximations. A discussion of the complexity of this system is given by Goldman et al. [3]. It might appear at first that a simple doubling of the rotational levels by the tunneling through the low trans barrier would give a useful approximation to the partition function. This is not sufficient because the tunneling induces a splitting which increases from  $\sim 11 \text{ cm}^{-1}$  (for  $n = 0$ ) to  $\sim 106.3 \text{ cm}^{-1}$  ( $n = 1$ ), to  $\sim 206 \text{ cm}^{-1}$  ( $n = 2$ ), etc. and the rotational constants ( $A, B, C, \Delta_K$ , etc.) vary significantly from one torsional state to another. For each rotational state, the energies for the torsional states are labeled by  $n$ . The analytical model developed considered all states up to  $n = 7$  and is based on Watson's analytical formula [6]. Vibrational partition sums were calculated using only the 5 “low amplitude modes,  $v_1, v_2, v_3$ , ( $A_{\text{gs}}$  symmetry) and the  $v_5, v_6$  ( $B_{\text{us}}$  symmetry), 3580, 1395.8, 865.939 37, 3780, and 1264.58417  $\text{cm}^{-1}$ , respectively, as suggested by the studies of Refs. [13–16]. The exact value of  $Q(T)$  calculated by direct sum at 296 K is 9851.664 73. The analytical model developed here gives 9819.750 19, a 0.3% difference.

Table 1 presents the total internal partition sum at 296 K for the species considered in this work. Also given in the table are the state-independent statistical factors, which are often needed when comparing with values from the literature.

Comparisons were made with data taken from the literature for at least the principal isotopologue of each molecule except HI and NO<sup>+</sup> for which no literature values were found. In total there are 98 comparisons made. For cases where the literature values are only for the rotational partition sum, the literature value is multiplied by the vibrational partition sum (product approximation) in order to compare with the TIPS calculated in this work. Most of the comparisons show very good agreement: the percent difference,  $100 * (Q_{\text{literature}} - Q_{\text{this work}})/Q_{\text{literature}}$ , for 83 comparisons are less than 1 percent, 14 are between 1 and 2 percent, and one is 4.75%. The last comparison, for C<sub>2</sub>H<sub>6</sub> at 300 K, demonstrates the need to add anharmonic corrections for torsion in ethane to our calculations. This is currently being pursued. The comparisons are presented in Ref. [10].

#### 4. Recall of data

Although some compilations of partition functions [1,2,17,18] utilized a four- or five-coefficient polynomial fit to the  $Q(T)$  data and provided the coefficients as a means of rapid recall, this work has abandoned that concept in favor of interpolation.

Table 1

Total internal partition sums at 296 K for molecular species on the HITRAN database

Molecule	ISO Code <sup>a</sup>	$Q_{\text{tot}}(296 \text{ K})$	$d_i$	Molecule	ISO Code <sup>a</sup>	$Q_{\text{tot}}(296 \text{ K})$	$d_i$
H <sub>2</sub> O	161	$1.7464 \times 10^2$	1	OH	61	$8.0362 \times 10^1$	2
	181	$1.7511 \times 10^2$	1		81	$8.0882 \times 10^1$	2
	171	$1.0479 \times 10^3$	6		62	$2.0931 \times 10^2$	3
	162	$8.5901 \times 10^2$	6		19	$4.1466 \times 10^1$	4
	182	$8.7519 \times 10^2$	6		15	$1.6066 \times 10^2$	8
	172	$5.2204 \times 10^3$	36		17	$1.6089 \times 10^2$	8
CO <sub>2</sub>	626	$2.8694 \times 10^2$	1	HCl	19	$2.0018 \times 10^2$	8
	636	$5.7841 \times 10^2$	2		11	$2.0024 \times 10^2$	8
	628	$6.0948 \times 10^2$	1		17	$3.8900 \times 10^2$	12
	627	$3.5527 \times 10^3$	6		56	$3.2746 \times 10^3$	4
	638	$1.2291 \times 10^3$	2		76	$3.3323 \times 10^3$	4
	637	$7.1629 \times 10^3$	12		622	$1.2210 \times 10^3$	1
	828	$3.2421 \times 10^2$	1		624	$1.2535 \times 10^3$	1
	728	$3.7764 \times 10^3$	6		632	$2.4842 \times 10^3$	2
	727	$1.1002 \times 10^4$	1		623	$4.9501 \times 10^3$	4
O <sub>3</sub>	666	$3.4838 \times 10^3$	1	OCS	822	$1.3137 \times 10^3$	1
	668	$7.4657 \times 10^3$	1		126	$2.8467 \times 10^3$	1
	686	$3.6471 \times 10^3$	1		136	$5.8376 \times 10^3$	2
	667	$4.3331 \times 10^4$	6		128	$2.9864 \times 10^3$	1
	676	$2.1405 \times 10^4$	6		165	$1.9274 \times 10^4$	8
	886	$7.8232 \times 10^3$	1		167	$1.9616 \times 10^4$	8
	868	$4.0063 \times 10^3$	1		44	$4.6598 \times 10^2$	1
	678	$4.5896 \times 10^4$	6		124	$8.9529 \times 10^2$	6
	768	$4.6468 \times 10^4$	6		134	$1.8403 \times 10^3$	12
	786	$4.5388 \times 10^4$	6		125	$6.2141 \times 10^5$	4
	776	$2.6630 \times 10^5$	36		1661	$9.8198 \times 10^3$	1
	767	$1.3480 \times 10^5$	1		215	$1.1583 \times 10^5$	4
	888	$4.2015 \times 10^3$	1		217	$1.1767 \times 10^5$	4
	887	$4.8688 \times 10^4$	6		1221	$4.1403 \times 10^2$	1
	878	$2.4640 \times 10^4$	6		1231	$1.6562 \times 10^3$	8
	778	$2.8573 \times 10^5$	36		1221	$7.0780 \times 10^4$	1
	787	$1.4126 \times 10^5$	1		1111	$3.2486 \times 10^3$	2
	777	$8.2864 \times 10^5$	6		1221	$1.3809 \times 10^3$	12
N <sub>2</sub> O	446	$5.0018 \times 10^3$	9	CH <sub>3</sub> CL	1221	$1.0712 \times 10^2$	1
	456	$3.3619 \times 10^3$	6		1221	$2.2408 \times 10^2$	2
	546	$3.4586 \times 10^3$	6		1221	$1.1247 \times 10^2$	1
	448	$5.3147 \times 10^3$	9		1221	$6.5934 \times 10^2$	6
	447	$3.0971 \times 10^4$	54		1111	$2.3582 \times 10^2$	2
					1111	$1.3809 \times 10^3$	12
CO	26	$1.0712 \times 10^2$	1	C <sub>2</sub> H <sub>2</sub>	1221	$4.1403 \times 10^2$	1
	36	$2.2408 \times 10^2$	2		1231	$1.6562 \times 10^3$	8
	28	$1.1247 \times 10^2$	1		1221	$7.0780 \times 10^4$	1
	27	$6.5934 \times 10^2$	6		1111	$3.2486 \times 10^3$	2
	38	$2.3582 \times 10^2$	2		1111	$1.3809 \times 10^3$	12
	37	$1.3809 \times 10^3$	12		1111	$1.3809 \times 10^3$	12

Table 1 (continued)

Molecule	ISO Code <sup>a</sup>	$Q_{\text{tot}}(296 \text{ K})$	$d_i$	Molecule	ISO Code <sup>a</sup>	$Q_{\text{tot}}(296 \text{ K})$	$d_i$
CH <sub>4</sub>	211	$5.9045 \times 10^2$	1	COF <sub>2</sub>	269	$7.0044 \times 10^4$	1
	311	$1.1808 \times 10^3$	2	SF <sub>6</sub>	29	$1.6233 \times 10^6$	1
	212	$4.7750 \times 10^3$	3				
O <sub>2</sub>	66	$2.1577 \times 10^2$	1	H <sub>2</sub> S	121	$5.0307 \times 10^2$	1
	68	$4.5230 \times 10^2$	1		141	$5.0435 \times 10^2$	1
	67	$2.6406 \times 10^3$	6		131	$2.0149 \times 10^3$	4
NO	46	$1.1421 \times 10^3$	3	HCOOH	126	$3.9133 \times 10^4$	4
	56	$7.8926 \times 10^2$	2	HO <sub>2</sub>	166	$4.3004 \times 10^3$	2
	48	$1.2045 \times 10^3$	3				
SO <sub>2</sub>	626	$6.3403 \times 10^3$		ClONO <sub>2</sub>	5646	$4.7884 \times 10^6$	12
	646	$6.3689 \times 10^3$	1		7646	$4.9102 \times 10^6$	12
NO <sub>2</sub>	646	$1.3578 \times 10^4$	3	NO <sup>+</sup>	46	$3.1168 \times 10^2$	3
NH <sub>3</sub>	4111	$1.7252 \times 10^3$	3	HOBr	169	$2.8339 \times 10^4$	8
	5111	$1.1527 \times 10^3$	2		161	$2.8238 \times 10^4$	8
HNO <sub>3</sub>	146	$2.1412 \times 10^5$	6	C <sub>2</sub> H <sub>4</sub>	221	$1.1041 \times 10^4$	1
					231	$4.5197 \times 10^4$	2

<sup>a</sup>HITRAN isotopologue/isotopomer code

The reasons for this transition are numerous. First, as available computer power and storage space constantly increase, it is no longer necessary to provide final data in the most terse manner possible. The entire set of tables as an uncompressed, fixed format file occupies only a few megabytes of storage space, and although the interpolation routines require somewhat more computer time than the polynomial expansion, both methods are nearly instantaneous in modern terms.

Second, when polynomial fits were used, there were a number of species for which the error introduced by the fits was greater than the 1% criterion at certain temperatures. Studies revealed that systems with many low lying vibrational states gave vibrational partition sums that increase rapidly. When the product with the rotational partition sum is made the resulting total internal partition sum increases too rapidly to fit accurately by the polynomial in the chosen temperature ranges. With interpolation of  $Q(T)$  data the situation is improved. The values produced by interpolation are, in general, much closer to the calculated values than those produced by polynomial expansion. Fig. 4 shows the error introduced by using interpolation with a step size of 50 K for nitric acid. Nitric acid was selected for this study because its partition function is difficult to fit by a polynomial function. As evidenced by these graphs, a step size of 50 K is more than satisfactory, even for a species which is troublesome to fit.

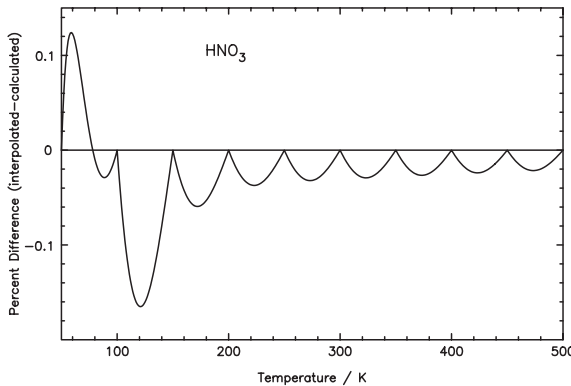


Fig. 4. Error in recalculated  $Q(T)$  by interpolation with 50 K step size for nitric acid.

A third reason for the switch to interpolation is that it presents the data in the most direct form possible. By looking at the tables, or using them as input data to a graphing program, it is possible to immediately see trends in the partition functions. Also, since the actual numbers are provided, rather than coefficients which are not directly meaningful, there is a much smaller chance of the wrong values being used in a calculation, or the accidental switching of two coefficients for example.

As part of this work, various interpolation schemes were considered. Since partition functions have a rather exponential trend, the concept of storing either  $\ln(Q(T))$  versus  $T$  or  $\ln(Q(T))$  versus  $\ln(T)$  was tested for the efficacy of reducing interpolation errors. Three schemes were tested; 4-point Lagrange interpolation of  $Q(T)$  versus  $T$ ,  $\ln\{Q(T)\}$  versus  $T$ , and  $\ln\{Q(T)\}$  versus  $\ln\{T\}$ . Fig. 5 shows the percent difference (calculated-interpolated) for the three schemes with 50 K temperature step for nitric acid. From the plot it is clear that the  $Q(T)$  versus  $T$  and  $\ln\{Q(T)\}$  versus  $\ln\{T\}$  interpolations are more precise than the  $\ln\{Q(T)\}$  versus  $T$  interpolation. Fig. 6 shows the maximum error at all points within the temperature range of interest for nitric acid, for the  $Q(T)$  versus  $T$  and  $\ln\{Q(T)\}$  versus  $\ln\{T\}$  interpolations as a function of the spacing between temperature points. As Fig. 6 shows, although taking the logarithm of both axes significantly reduces the maximum error at large step-size values, it does little, or even increases the error at smaller step-size values. Additionally, providing tables of  $\ln(Q(T))$  versus  $\ln(T)$  still makes it difficult to examine the data without performing further calculations. In light of all of these findings, and a critical analysis of the size of the tables required versus induced error, the decision was made to use interpolation with a 25 K step size and no logarithms.

Data tables were generated that list values for  $Q(T)$  at 25 K intervals. A four-point Lagrange interpolation scheme is used, with extra points provided below 70 K and above 3000 K so that a four point interpolation can be used throughout the entire temperature range. These tables and the four-point Lagrange interpolation scheme were then coded into a FORTRAN program (TIPS\_2003.for) and subroutine (BD\_TIPS\_2003.for) and are available from one of the authors (RRG, see [faculty.uml.edu/Robert\\_Gamache](http://faculty.uml.edu/Robert_Gamache)) or the HITRAN ftp site ([cfa-ftp.harvard.edu/publ/HITRAN](http://cfa-ftp.harvard.edu/publ/HITRAN)).

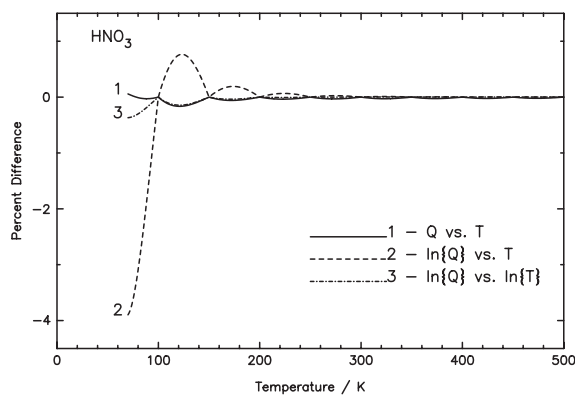


Fig. 5. Error in recalculated  $Q(T)$  by different interpolation schemes with 25 K step size for nitric acid. (a)  $Q$  vs.  $T$ , (b)  $\ln\{Q\}$  vs.  $T$ , and (c)  $\ln\{Q\}$  vs.  $\ln\{T\}$ .

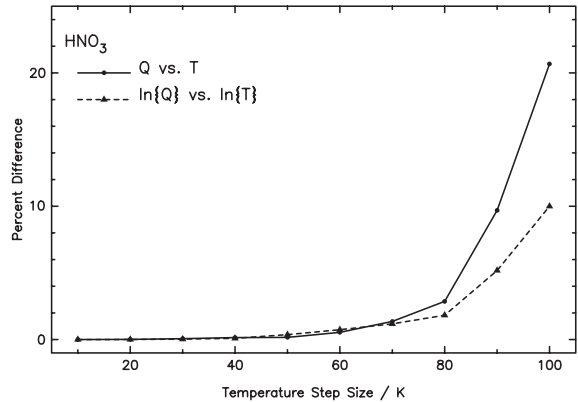


Fig. 6. Error versus temperature step size in interpolation for  $Q(T)$  vs.  $T$  (solid circles) and  $\ln\{Q(T)\}$  vs.  $\ln\{T\}$  (triangles) for nitric acid.

## 5. Discussion

The partition sums calculated above include all isotopologues/isotopomers on the HITRAN database as well as some isotopologues/isotopomers not currently on the database. The partition sums are provided in tabular form with a 25 K step size, accompanied by a Lagrange interpolation program to evaluate the partition sums at any temperature within the temperature range of this study. The conversion to an interpolation scheme has allowed for the inclusion of a number of partition sums which were previously undistributed because they could not be fit with a suitable degree of accuracy by the polynomial expression used at that time.

Although this work is similar to previously released partition functions, it also includes many new species, several new analytical models, interpolation for greater accuracy, and incorporates all of the corrections to the previous set of partition functions discussed in Goldman et al. [3]. There are a number of improvements that will be made to the partition sums in the future. For molecular systems where it is necessary to use the product approximation this work only included the harmonic oscillator approximation of Herzberg [9]. Anharmonic corrections will be added to the model for ethane. The analytical approximation of the rotational partition sum for asymmetric rotors [19] includes a component for centrifugal distortion that was not applied in this work.

## Acknowledgements

The authors would like to acknowledge Alain Barbe for providing constants for rare, isotopically substituted species of ozone. Two of the authors (J.F. and R.R.G.) are also pleased to acknowledge the support of this research by the National Science Foundation Grant No. ATM-9812540, and the University of Massachusetts Lowell Council on Teaching, Learning and Research as Scholarship. Any opinions, findings, and conclusions or recommendations expressed in this material are those of the author(s) and do not necessarily reflect the views of the National Science Foundation.

## References

- [1] Gamache RR, Hawkins RL, Rothman LS. Total internal partition sums in the temperature range 70–3000 K: atmospheric linear molecules. *J Mol Spectrosc* 1990;142:205–19.
- [2] Gamache RR, Kennedy S, Hawkins R, Rothman LS. Total internal partition sums for molecules in the terrestrial atmosphere. *J Mol Struct* 2000;517–518:413–31.
- [3] Goldman A, Gamache RR, Perrin A, Flaud J-M, Rinsland CP, Rothman LS. HITRAN partition functions and weighted transition-moments squared. *JQSRT* 2000;66:455–86.
- [4] Rothman LS, Barbe A, Benner DC, Brown LR, Camy-Peyret C, Carleer MR, Chance KV, Clerbaux C, Dana V, Devi VM, Fayt A, Flaud J-M, Gamache RR, Goldman A, Jacquemart D, Jucks KW, Lafferty WJ, Mandin J-Y, Massie ST, Nemchinov V, Newnham DA, Perrin A, Rinsland CP, Schroeder J, Smith KM, Smith MAH, Tang K, Toth RA, Vander-Auwera J, Varanasi P, Yoshino K. The HITRAN molecular spectroscopic database: edition of 2000 including updates through 2001. *JQSRT* doi:10.1016/S0022-4073(03)00146-8.
- [5] McDowell RS. Rotational partition functions for linear molecules. *J Chem Phys* 1988;88:356–61.
- [6] Watson JKG. The asymptotic asymmetric-top rotational partition function. *Mol Phys* 1988;65:1377–97.
- [7] McDowell RS. Rotational partition functions for spherical-top molecules. *JQSRT* 1987;71:414–29.
- [8] McDowell RS. Rotational partition functions for symmetric-top molecules. *J Chem Phys* 1990;93:2801–11.
- [9] Herzberg G. Molecular spectra and molecular structure II. Infrared and Raman spectra of polyatomic molecules. New York: Van Nostrand, 1960.
- [10] Fischer J, Gamache RR, Goldman A, Rothman LS, Perrin A. Total internal partition sums for molecular species on the HITRAN database. Scientific report No. AS03-01, Department of Environmental, Earth, and Atmospheric Sciences, University of Massachusetts Lowell, 2003.
- [11] Beaudet RA, Poynter RL. Mirowave spectra of molecules of astrophysical interest. XII. Hydroxyl radical. *J Phys Chem Ref Data* 1978;7:311–3.
- [12] Perrin A, Flaud J-M, Camy-Peyret C, Carli B, Carlotti M. The far infrared spectrum of  $^{14}\text{N}^{16}\text{O}_2$ . Electron spin-rotation and hyperfine Fermi contact resonances in the ground state. *Mol Phys* 1988;63:791–810.
- [13] Flaud J-M, Camy-Peyret C, Johns JWC, Carli B. The far infrared spectrum of  $\text{H}_2\text{O}_2$ . First observation of staggering of the levels and determination of the *cis* barrier. *J Chem Phys* 1989;91:150–1.
- [14] Perrin A, Flaud J-M, Camy-Peyret C, Schernaul R, Winnewisser M, Mandin J-Y, Dana V, Badaoui M, Koput J. Line intensities in the far infrared spectrum of  $\text{H}_2\text{O}_2$ . *J Molec Spectrosc* 1996;176:287–96.
- [15] Flaud J-M, Perrin A. High-resolution infrared spectroscopy and one dimensional large amplitude motion in asymmetric tops:  $\text{HNO}_3$  and  $\text{H}_2\text{O}_2$ . In Papousek D, editor. *Vibration-Rotational Spectroscopy & Molecular Dynamics*, Advanced series in physical chemistry, Vol. 9. Singapore: World Scientific Publishing Co., 1997. p. 396–460 [chapter 7].
- [16] Klee S, Winnewisser Perrin A, Flaud J-M. Absolute line intensities for the  $v_6$  band of  $\text{H}_2\text{O}_2$ . *J Molec Spectrosc* 1999;195:154–61.
- [17] Fischer J, Gamache RR. Total internal partition sums for molecules of astrophysical interest. *JQSRT* 2001;74: 263–73.
- [18] Fischer J, Gamache RR. Partition sums for non-local thermodynamic equilibrium applications. *JQSRT* 2001;74: 273–84.
- [19] Watson JKG. Determination of centrifugal distortion coefficients of asymmetric-top molecules. *J Chem Phys* 1967;46:1935–49.